World Academy of Science, Engineering and Technology
International Journal of Electrical and Computer Engineering
Vol:7, No:6, 2013

Analysis of the Root Causes of Transformer Bushing Failures

E. A. Feilat, I. A. Metwally, S. Al-Matri, and A. S. Al-Abri

***Abstract*—**This paper presents the results of a comprehensive investigation of five blackouts that occurred on 28 August to 8 September 2011 due to bushing failures of the 132/33 kV, 125 MVA transformers at JBB Ali Grid station. The investigation aims to explore the root causes of the bushing failures and come up with recommendations that help in rectifying the problem and avoiding the reoccurrence of similar type of incidents. The incident reports about the failed bushings and the SCADA reports at this grid station were examined and analyzed. Moreover, comprehensive power quality field measurements at ten 33/11 kV substations (S/Ss) in JBB Ali area were conducted, and frequency scans were performed to verify any harmonic resonance frequencies due to power factor correction capacitors. Furthermore, the daily operations of the on-load tap changers (OLTCs) of both the 125 MVA and 20 MVA transformers at JBB Ali Grid station have been analyzed. The investigation showed that the five bushing failures were due to a local problem, i.e. internal degradation of the bushing insulation. This has been confirmed by analyzing the time interval between successive OLTC operations of the faulty grid transformers. It was also found that monitoring the number of OLTC operations can help in predicting bushing failure.

***Keywords*—**Modeling and simulation, power system, transformer, bushing, OLTC, power quality, partial discharge.

I. Introduction

TRANSFORMERS are important components in electrical power systems and represent very large investments. The effects of failures in terms of loss of revenue, outage time and cost of financing repairs are critical in modern power systems and have serious effects on operational performance. Transformer failure analysis shows in average about 10% of transformer failures are caused by bushings damage which is often followed with catastrophic consequences [1]. This percent is essentially more for large transformers.

Five incidents of transformer-bushing failures occurred at JBB Ali Grid station on 28 August to 8 September 2011. Some of these incidents resulted in bushing explosion of the porcelain housing and its head. The transformers were in service since 2001 and they were running satisfactorily till the first Bushing failure which occurred after 10 years. A summary of the five incidents are presented in Table I. Mazoon Electricity Company along with consultants undertook detailed study to find root cause of failures.

E. A. Feilat and I. A. Metwally are with the Department of Electrical & Computer Engineering Sultan Qaboos University, Muscat, Oman (metwally@squ.edu.om).

S. Al-Matri and A. S. Al-Abri are with Mazoon Electricity Company, P.O. Box 1229, Hamriya P.C 131, Oman.

To identify the root cause of the Grid station transformer bushing repeated failures, physical inspection and detailed simulation studies were conducted. The physical inspection includes viewing and analyzing the layers of the condenser foil and its paper insulation, installation practice, grounding points, maintenance records and tap changer operation. A visual inspection of the failed bushings is shown in Fig. 1, where there are burn-through marks on the bushing condenser paper and two melted spots on the HV central lead. These observations are considered as good indicators of localized internal insulation breakdown.

In this paper, comprehensive power quality measurements and detailed simulation studies covering lightning overvoltage and harmonic resonance studies were carried. This paper aims to:

- investigate the root causes for transformer-bushing failures at JBB Ali Grid station,
- identify the possible mechanisms or events that have resulted in the incidents,
- identify any test or additional system monitoring that should be undertaken to increase the understanding of the failure mechanism, and
- provide recommendations to effectively and efficiently minimize the risk of such incidents in the future.

TABLE I
Summary of Transformer Incidents at JBB Ali Grid S/S

Date & Time	TX-1	TX-2	Grid S/S Configuration
28/08/2011 19:10Hrs	On Service	**Tripped** 33 kV Y-ph bushing failed	Full load of JBB ALI carried by TX1
3/9/2011 19:25Hrs	**Tripped** 33 kV Y-ph bushing failed	Out of Service	**Black Out** TX 2 out of service
4/9/2011 13:26Hrs	Out of service	Energized	TX2 in service, full load restored
5/9/2011 07:36Hrs	Out of service	**Tripped** 33 kV Y-ph bushing failed	**Black Out** TX1 out of service.
6/9/2011 04:20Hrs	Out of service	Energized	TX2 in service, load restored
7/9/2011 02:19Hrs	Energized	On Service	TX1 & TX 2 in service.
7/9/2011 18:33Hrs	On Service	**Tripped** 33 kV B-ph bushing failed	On Service
8/9/2011 19:48Hrs	**Tripped** 33 kV R-ph bushing failed	Energized without load	Load restored through TX 2
9/9/2011	Energized at 16:35Hrs	On service	TX1 & TX 2 in service

Fig. 1 Photo of three failed transformer bushings

II. Bushing Failure Mechanisms and Facts

A. Construction and Diagnosis of Condenser Bushings

Two common types of transformer bushings are used, namely, solid porcelain bushing for smaller transformers and oil filled condenser bushings for larger transformers (also called oil impregnated paper (OIP) bushing). Solid porcelain bushings consist of high grade porcelain cylinders that conductor pass through. Outside surface have a series of skirts to increase the leakage path distance to the grounded metal case. High voltage bushing is generally oil filled condenser type. The construction details of a typical condenser bushing rated ≤69 kV are presented in Fig. 2 [2]. Condenser types have a central conductor wound with alternating layers of paper insulation and tin foil and filled with insulating oil. Each conductive layer acts as a condenser and voltage equalizer. This results in a path from the conductor to the grounded tank, consisting of a series of condensers. The layers are designed to provide approximately equal voltage drops between each condenser layer. This kind of bushing is.

Failure of OIP bushings can be avoided by detecting the defect or degradation of bushings caused by the stresses acting on them in time. This can be done by applying diagnostic techniques for bushings such as: visual inspection, infrared scanning, DC insulation resistance test, capacitance and power factor (*tanδ*) measurement, PD test, oil sampling, etc. Capacitance and power factor (*tanδ*) measurement is an important diagnostic method to detect critical degradation caused by many problems including moisture penetration.

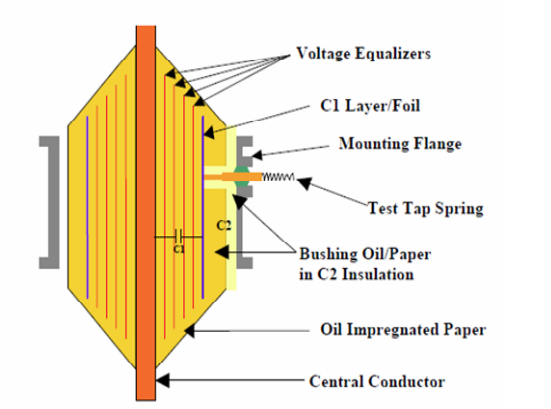

Fig. 2 Construction of typical OIP condenser bushing rated ≤69 kV[2]

B. Bushing Failure Mechanisms

Failure of power transformer results in a serious damage to assets and reliability of the power system. In addition to the OLTC and transformer windings, the bushing is one of the major components causing forced outages of power transformer. A CIGRE international survey [1, 3] indicated that the most frequent sources of transformer failures can be attributed to the tap changers, bushings, the paper-oil insulation and the accessory equipment. Experience and testing of failed transformer bushings revealed the following facts about transformer busing failures:

- HV bushing is one of the transformer components responsible for more than 30% of transformer failures.
- Insulation failures were the leading cause of transformer failures.
- Heat, oxidation, acidity, and moisture are main factors that are responsible for insulation deterioration.
- Inadequate or improper maintenance and operation was a major cause of transformer failures.
- Experience has shown that dielectric withstand strength of the oil part of HV bushing could be very sensitive to contamination of transformer oil with conductive particles due to deposit of carbon on the lower porcelain surface.

Similarly, transformer bushings encounter current and temperature stresses due to short circuits and heavy loading conditions. As a result, the multilayer bushing insulation expands under high temperature due to high loading condition. On the other hand, during cooling the multilayer shrink and create miniature gaps. This process helps moisture penetration into the bushing through leaky gaskets or other openings. Moisture penetration is usually associated with partial discharge activity causing degradation across the internal surface of bushing. Furthermore, environmental pollution lead to degradation of bushings and finally to failure.

III. Possible Failure Mechanisms of JBB Ali Grid Transformer 33 kV Bushing

During daily operation, condenser bushings of transformers encounter overvoltage stresses acting on them e.g. voltage stress due to harmonic resonance or switching overvoltage transient resulting from capacitor switching or abnormal OLTC operations. As a result, partial discharge activity inside the multilayer insulation of the bushing is accelerated which result in unforeseen bushing failure.

Similarly, overvoltages could occur as a result of switching transients due to capacitor switching [4, 5], of power factor correction capacitor, or any abnormal operation of the 132 kV OLTC. In this regard, if the overvoltage transient is initiated at the 132 kV OLTC, will propagate towards downstream to the 33 and 11 kV voltage levels until it is damped due to resistances of the transformers, cables and overhead lines. On the other hand, if the overvoltage transient occurred at the capacitor banks, it will propagate towards upstream from the 11 kV level to the 33 and 132 kV voltage levels.

Statistical analysis of the faulty operation of the OLTCs of JBB Ali Grid S/S is depicted in Fig. 3. Fig. 3 shows the time

interval between OLTC successive operations for the faulty JBB Ali Grid transformer. The results indicate that the OLTC time intervals are too small which implies an abnormal operation as a result of frequent variation of the 33 kV voltage level of the 125 MVA transformers. This fast variation could be attributed to successive partial discharges activities in the bushing insulation.

IV. Power Quality Field Measurements

Application of capacitor banks for power factor control and reduction of reactive power flow on the power system can create series or parallel resonance, which magnifies the problem of harmonic current distortion produced by nonlinear loads. If the resonant frequency is near one of the harmonic currents produced by the non-linear loads, a high-voltage distortion can take place. To limit both voltage and current harmonic distortion, the IEEE Standard 519-1992 [6] proposes to limit harmonic current injection from end users so that harmonic voltage levels on the overall power system will be acceptable This approach requires participation from both end users and utilities [6].

The most commonly used two indices for measuring the harmonic content of a waveform are the total harmonic distortion (THD) and the total demand distortion (TDD). Both are measures of the effective value of a waveform and may be applied to either voltage or current. Most utilities impose limits on the amount of harmonic current that can be injected onto the utility system. This is done to ensure that relatively harmonic-free voltage is supplied to all customers on the distribution line. IEEE Standard 519-1992 recommends limits for harmonics for both utilities and customers at the point of common coupling (PCC) or a point of metering for direct measurement of the harmonic indices. The recommended levels vary depending on the size of the load with respect to the size of the power system, and also upon the voltage at PCC. The voltage and current THD is defined as [5, 6]:

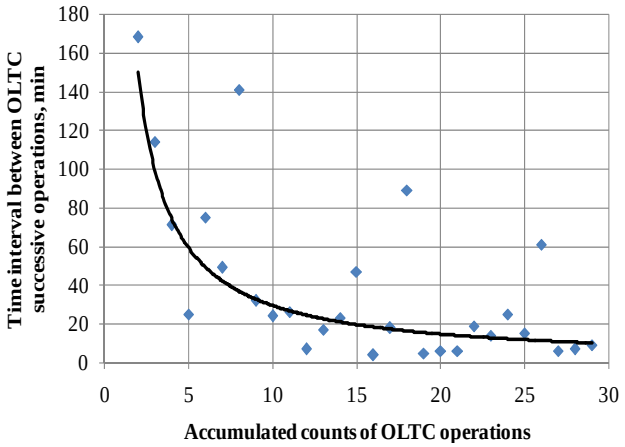

Fig. 3 JBB Grid station, TX1, 8-9-2011

$$THD_V = \frac{\sqrt{\sum_{h=2}^{h_{max}} V_h^2}}{V_1} = \frac{\sqrt{\left(V_2^2 + V_3^2 + \cdots V_{h\max}^2\right)}}{V_1} \times 100\% \quad (1)$$

The total demand distortion index (TDD) concept was created to better relate the current THD to the maximum load current. The compliance with recommended levels keeps harmonic current penetration into the distribution system under control [5, 6].

$$TDD = \frac{\sqrt{\sum_{h=2}^{h_{max}} I_h^2}}{I_L} \times 100\% = \frac{\sqrt{\left(I_2^2 + I_3^2 + \cdots I_{h\max}^2\right)}}{I_L} \times 100\% \quad (2)$$

The IEEE 519 guidelines do not specify a definite measurement period for capturing harmonic waveform distortion. Under steady-state operation, where no loading variations occur, a few minutes recording may be sufficient and averaging over a few seconds should meet the requirements. However, due to the changing nature of loads in most situations, measurements over a few days may be needed to assure that load variation patterns and their effects on harmonic distortion are considered. IEC 61000-2-2 9 suggests assessment periods of one week.

From the electric utility perspective, the general objectives for conducting harmonic measurements may be summarized as follows:

- To verify the order and magnitude of harmonic currents at the S/S and at remote locations where customer harmonic sources may be affecting neighboring installations.
- To determine the resultant waveform distortion expressed in the form of spectral analysis.
- To compare the preceding parameters with recommended limits or planning levels.
- To assess the possibility of network resonance that may increase harmonic distortion levels, particularly at or near capacitor banks.

A. PQ Measurements at MZEC Substations

In this study, power quality (PQ) measurements were conducted at 10 indoor and outdoor S/Ss that owned by MZEC. In addition, PQ measurements were conducted at the JBB Ali Grid S/S as well. For the indoor S/Ss, the PQ meters were hooked for a period of one week, whereas for the outdoor S/Ss the PQ meters were connected for a period of 5 minutes. The PCC points were chosen at 132 kV bus for the 132/33 kV Grid S/Ss and at the 11 kV for the 33/11 kV indoor and outdoor S/Ss. The CTs and VTs available at the S/Ss were used for the PQ measurements.

Two types of PQ meters were used for measurements, namely AEMC 3945B PowerPad 3-Phase Power Quality Analyzer and Power Sight PS4500 Power Quality Analyzer. Likewise, the grounding resistance was measured using AMEC 3711 Clamp-On Ground Resistance Tester. A number of indicators are used to quantify and evaluate the harmonic

distortion in current and voltage waveforms, namely grounding resistance (R_g), frequency, line voltages and currents, *THDV* and *THDI* indices, power factor, real, reactive and apparent power, voltage and current unbalance, crest factor, and percentage individual voltage and current harmonic magnitudes.

TABLE II
SAMPLES OF AVERAGE VALUES OF MEASURED PQ QUANTITIES

Measured quantity	Substation Name	JalanBani Bu Ali Grid (2x125MVA)		BBC (2 X10MVA)	JalanBani Bu Ali Primary (2 x20MVA)		JalanBani Bu Ali Grid MZEC (2x20MVA)	
	Unit	TX1	TX2	TX	TX1	TX2	TX1	TX2
f	(Hz)	49.98	49.98	50.02	50.01	50.02	50.00	50.03
PF	(pu)	0.992	0.984	0.83	0.986	0.979	0.900	0.940
I	A (A)	60.16	60.33	15.92	94.90	140.39	49.49	82.99
	B (A)	54.89	57.22	14.63	94.50	136.03	54.61	66.28
	C (A)	54.83	55.37	15.18	105.70	138.15	53.90	73.48
V	AB (kV)	134.40	129.26	32.70	11.58	11.73	11.67	11.57
	BC (kV)	133.58	127.92	32.75	11.58	11.72	11.67	11.58
	CA (kV)	133.68	133.69	32.80	11.60	11.74	11.67	11.59
CU	(%)	3.52	3.91	5.17	6.66	1.60	6.41	14.00
VU	(%)	0.40	2.70	0.18	0.04	0.10	0.01	0.10
C-THD	A (%)	3.13	3.43	4.58	8.80	5.12	11.35	6.25
	B (%)	2.78	3.14	5.95	8.80	5.23	11.38	7.46
	C (%)	3.36	3.35	4.20	8.10	5.83	11.25	6.46
V-THD	AB (%)	1.00	0.90	1.78	1.30	1.41	3.81	2.10
	BC (%)	1.02	0.90	1.66	1.30	1.48	3.87	2.00
	CA (%)	0.94	0.92	1.65	1.10	1.17	3.76	1.91
C-CF	A (pu)	1.40	1.40	1.48	1.47	1.50	1.50	1.46
	B (pu)	1.42	1.43	1.40	1.51	1.48	1.60	1.50
	C (pu)	1.44	1.44	1.43	1.46	1.46	1.50	1.47
V-CF	AB (pu)	1.43	1.43	1.41	1.43	1.43	1.40	1.44
	BC (pu)	1.43	1.43	1.41	1.42	1.42	1.40	1.42
	CA (pu)	1.43	1.43	1.42	1.43	1.43	1.40	1.44
TDD	(%)	0.58	0.63	3.10	1.12	0.74	3.11	1.03
IEEE 519	(%)	2.5	2.5	8.0	5.0	5.0	8.0	8.0
IEEE Compliance		Yes	Yes	Yes	Yes	Yes	Yes	Yes
R_g	(Ω)	≤ 0.35		≤ 0.08	≤ 0.7		≤ 0.6	

The grounding resistance (R_g) has been measured at different grounding locations in the S/Ss (TX1, TX2, Aux. TX, Capacitor Banks, and Surge Arresters). However, the highest reading was considered. Table II shows that in most of the grounding locations the resistance was too small and below 1 Ω. Samples of weakly average values of the PQ measured quantities at the indoor S/Ss are given in Table II. For the outdoor S/Ss, 5-minute average values of the PQ measured quantities are provided. The results show that most of the measured data are with the international standard limits.

The values of TDDs were calculated based on the measured harmonic current levels and the maximum load currents at each S/S. The maximum load currents for balanced load condition were calculated by running the ETAP [7] load flow program at the summer peak load as provided by MZEC. The TDD limits are determined based on the ratio of the short-circuit level to the maximum load current (I_{sc}/I_L).

The average of weakly monitored harmonic voltages at JBB Ali 33/11 kV Grid S/S shows that the highest harmonic level is the 5th harmonic voltage which was around 2.4% and the other harmonic voltages are negligible.

Likewise, ETAP short-circuit current program has been used for calculating the short-circuit levels at the PCC of each S/Ss. The calculations of the TDD at the PCC of the above ten S/Ss indicate that the voltage and current harmonic distortion levels meet the IEEE519 standards limits and the TDD indices also show compliance with IEEE 519 Standard as illustrated in Table III.

B. Frequency Scan And Harmonics Resonance

A frequency scan of the system looking from the PCC is usually performed to detect the dominant parallel resonance frequency at which harmonic distortion is magnified. When the frequency components produced by a nonlinear load line up with the system natural frequency, the distortion will be magnified as given by

$$V_h = I_h Z_R \tag{3}$$

where I_h and V_h are the harmonic current and voltages at the resonant frequency, and Z_R is the impedance seen by the harmonic current source at the resonant frequency.

Impedance scan has been performed on the MZEC distribution system for JBB Ali area. The frequency scan was performed using Matlab software after representing the distribution system as seen from the PCC by the system short circuit impedance Z_{sc}. By applying (4) the resonance harmonic frequency can be determined [5, 8].

$$h_r = \sqrt{\frac{X_C}{X_L}} = \sqrt{\frac{kVA_{sc}}{kVAR_{cap}}} \approx \sqrt{\frac{kVA_{TX} \times 100}{kVAR_{cap} \times Z_{TX(\%)}}} \tag{4}$$

where h_r is the resonant frequency order, KVA_{SC} is the short-circuit power available at the site, $kVAR_{cap}$ is the reactive power rating of the capacitor bank and kVA_{TX} is transformer rating.

In this study, the impedance scan as seen by the PCC at the

TABLE III
IEEE COMPLIANCE OF TDD INDICES AT THE PCC OF THE MONITORED S/SS

Measured quantity	Substation Name	132 kV JalanBani Bu Ali Grid -One Bus- (2x125MVA)		33 kV JalanBani Bu Ali Grid -Two buses - (2x125MVA)		33 kV JalanBani Bu Ali Grid MZEC (2x20MVA)		11 kV JalanBani Bu Ali Grid MZEC (2x20MVA)		Al Ashkhara 11 kV (2 x10MVA)		BBC 33 kV (1 X10MVA)	WADI SALL 11 kV (3 X 6MVA)	
	Unit	TX1	TX2	TX1	TX2	TX3	TX4	TX1	TX2	TX1	TX2	TX	TX1	TX2
I_{Lmax}	A	300.3	300.3	1087.8	1250	63.6	144.8	214.6	486.8	260.3	265.9	36.20	170.2	139.8
Isc	kA	3.1	3.1	14.6	15.2	14.4	15.0	10.1	11.7	3.7	3.7	1.50	3.5	3.7
I_{sc}/I_{Lmax}		10.32	10.32	13.42	12.16	226.42	103.59	47.06	24.03	14.21	13.92	41.44	20.56	26.47
Calculated TDD	%	0.58	0.63	N/A	N/A	N/A	N/A	3.11	1.03	0.90	1.53	3.10	0.70	0.86
IEEE 519-Std. Value	%	2.5	2.5	5.0	5.0	15.0	15.0	8.0	8.0	5.0	5.0	8.0	8.0	8.0
IEEE Compliance		Yes	Yes					Yes	Yes	Yes	Yes	Yes	Yes	Yes

11 kV-bus where the capacitor banks are located has been computed for the ten S/Ss. Fig. 4 displays the frequency scan for Al Kamel water pump S/S. The results indicate that there is a possibility of resonance at the 5th and 7th harmonic frequencies. Therefore, if either the 5th or 7th harmonic current exists, the corresponding magnified harmonic voltage will be superimposed on the 50-Hz 11-kV bus.

Examining Fig. 4, it can be seen that harmonic parallel resonance at Al Kamel water pump S/S-TX1 is possible at the 5th and 7th harmonic frequencies corresponding to 3 and 1 MVAR compensation, respectively. The overall impedances of the combination of the capacitor bank and system equivalent short-circuit reactance as seen from the PCC Z_{R5}= 90 kΩ Z_{R7}= 34 kΩ, respectively. For 5th and 7th harmonic currents I_{h5} =2.3% and I_{h7} =0.7%, with I_{h1}=24 A, the corresponding magnitudes of the magnified 5th and 7th harmonic voltages are V_{h5} =75% and V_{h7} =86%, respectively. However, the damping provided by resistance in the system and the overvoltage surge arresters are often sufficient to prevent catastrophic voltages and currents.

V. ON-LOAD TAP-CHANGER (OLTC) OPERATION

The frequency of operations of the OLTCs of TX1 and TX2 of the 132/33 kV 125 MVA transformers at JBB Ali Grid S/S is compared to that of the healthy Sur Grid S/S during the time interval from 24/08/2011 to 16/09/2011 as depicted in Fig. 5. It can be seen that the OLTC of either Sur transformers (TX1 or TX2) hourly operation (i.e. number of tap changers operations per hour) are within the normal network operations i.e. 20 operations per day or <0.83 operations/hour [9]. On the other hand, the OLTC of either TX1 or TX2 at JBB Ali Grid S/S exhibits abnormal hourly operations i.e. above the normal network. This abnormal operation appeared on 27/08/2011 and 28/08/2011, which resulted in failure of TX2 on 28/08/2011 and TX1 on 03/09/2011, respectively.

This average number of operations was within the known operation range for normal networks [9] even after switching on the 11 kV capacitor banks at JBB Ali grid S/S to the auto mode. No significant effect of switching on the capacitor banks on OLTC operations per day in Dec. 2011 and Jan. 2012.

Likewise, another severe abnormal operation that exceeds the unstable network i.e. 30 operations/day or >1.25 operation/hour was observed on 04/09/2011. As a result, TX2 failed on 05/09/2011. These abnormal operations continued and yielded to two failures of TX2 on 07/09/2011 and TX1 on 08/09/2011, respectively even after switching off the capacitor banks at the 11.5 kV bus of MZEC JBB Ali 33/11.5 kV S/S.

For the sake of comparison, Fig. 6 shows the frequency of transformer OLTC operations at different 33/11.5 kV MZEC S/Ss including Sur Grid, JBB Ali Grid, JBB Ali primary and Shariya S/S in 2009, 2010 and 2011. It can be seen that TX3 transformer at JBB Ali Grid S/S exhibiting abnormal operation since 2010, where the number of daily operations

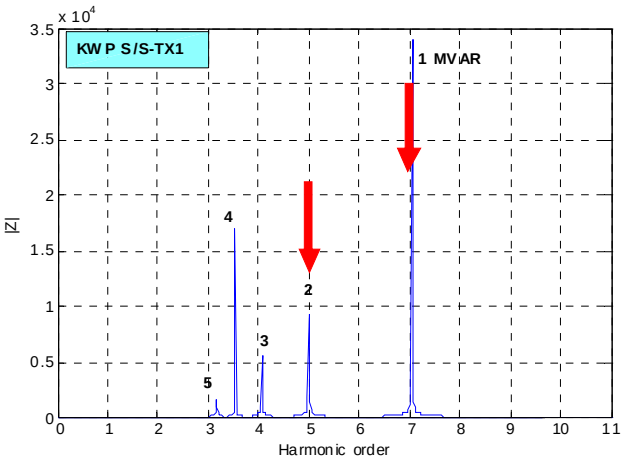

Fig. 4 Impedance scan- Al Kamel water pump S/S (TX1)

exceeds 20indicating unstable network operations at the JBB Ali Grid S/S.

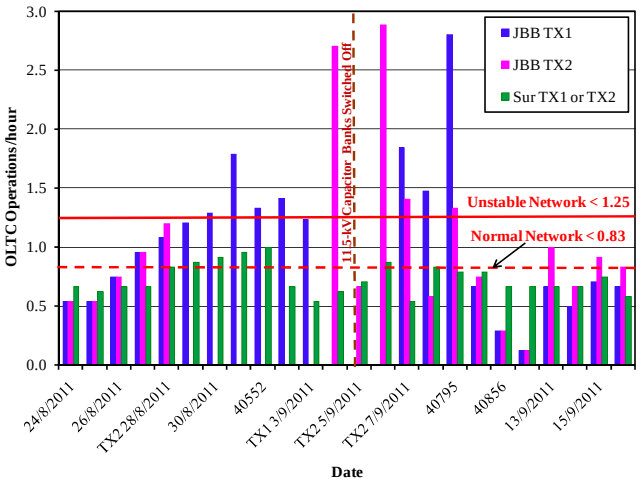

Fig. 5 Hourly-operations 132-kV OLTC at JBBA and Sur Grid S/Ss

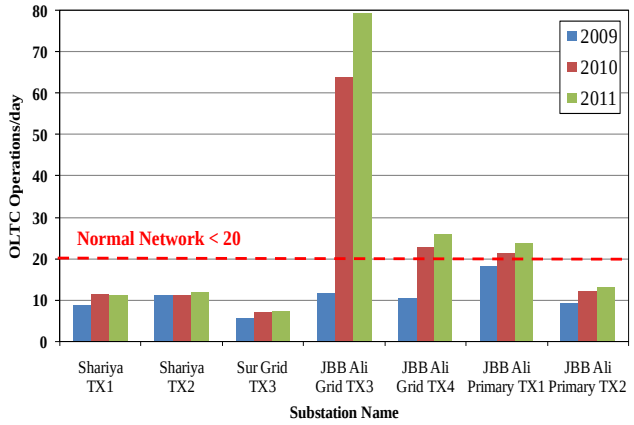

Fig. 6 Average daily operations of 33-kV OLTC in 2009, 2010 and 2011

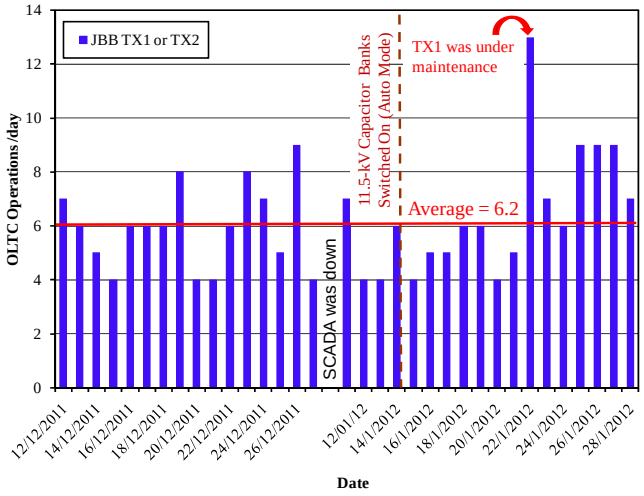

Fig. 7 Hourly 132-kV OLTC at JBB Grid S/S in Dec. 2011 and Jan. 2012 before and after switching-on of the 11.5-kV capacitor banks

Following the five failures of TX1 and TX2, the six 33 kV bushings were replaced. Accordingly, the daily operations of the OLTCs of both TX1 and TX2 during the time interval from 12/12/2011 to 28/01/2012 fall within the stable network operation as demonstrated in Fig. 7. The average daily operations was 6.2 operations/day or 0.26/hour.

VI. Conclusions

A comprehensive investigation of the five blackouts that occurred on 28 Aug. to 8 Sept. 2011 due to bushing failures of the 132/33 kV, 125 MVA transformers at JBB Ali Grid S/S was carried out. This extensive investigation includes inspection of the failed bushings, comprehensive power quality measurements, frequency scan, and OLTC daily operations. Based on the results of the proposed investigations and the visual inspection of failed bushings, it can be concluded that the failure is attributed to internal localized insulation breakdown as indicated by the burn-through marks on the condenser paper and two melted spots on the HV central conductor. All transformer bushings must be tested for $tan\delta$ and capacitance values at suitable intervals and adequate provision for spare bushings must be made for replacements.

It was also found that monitoring the number of OLTC operations can help in predicting bushing failure when it exceeds a threshold value of 20 operations per day or a monthly average of 10 operations.

Acknowledgment

The authors wish to express their appreciation to Sultan Qaboos University and Mazoon Electricity Company for supporting this research work.

References

[1] CIGRE-WG 12-05: An international survey on failures in large power transformers in service, Electra No. 88 1983, S. 21-48.

[2] P. Singh, "C_2 Power factor and capacitance of ABB type O plus C, AB, and Type T condenser bushings," Doble Client Conference Paper, 2001.

[3] I. A. Metwally, "Failures, monitoring, and new trends of power transformers," IEEE Potentials, May/June 2011, pp. 36-43.

[4] T. E. Grebe, "*Application of distribution system capacitor banks and their impact on power quality,*" IEEE Trans. Industry Applications, Vol. 32, No. 3, May/June 1996, pp. 714-719.

[5] R. C. Dugan, M. F. McGranaghan, S. Santoso, and H. W. Beaty, *Electrical Power Systems Quality*, Second Edition, McGraw-Hill, 2004.

[6] *IEEE Recommended Practices and Requirements for Harmonic Control in Electric Power Systems*, IEEE Std. 519-1992.

[7] ETAP-7.5 power system software. Operation Technology, Inc., Irvine, CA, http://www.etap.com.

[8] G. Brunello, B. Kasztenny, and C. Wester, "Shunt capacitor bank fundamentals and protection," 2003 Conference for Protective Relay Engineers, Texas A&M University, April 8-10, 2003, College Station (TX), USA.

[9] ABB Components, "On-load tap-changers for industrial applications," Available: http://www.estecegypt.com/power/ABB/tap_changers/.